formula for free precession of the electrons in a magnetic field, we obtain $\chi_\pi = -60(e^2/4m_e c^2)\langle\rho^2\rangle$, where $\langle\rho^2\rangle$, the expectation value of the mean square radius of the electron orbits is given by $2r^2/3 = 4.09l^2$. Thus the free electron theory gives $\chi_\pi^{C_{60}}/|\chi_\pi^{benzene}| = -(60/6)(4.09) = -40.9$ (strong diamagnetism). The quantum-mechanical London calculation presented earlier shows that the correct value is less than one-hundredth of the classical value.

Although planar aromatic hydrocarbons and graphite have provided appropriate points of analogy for the π-electron energy structure of C_{60}, it is clear that the magnetic response of C_{60} is unlike that of any other molecule yet encountered.

1. Kroto, H. W., Heath, J. R., O'Brien, S. C., Curl, R. F. & Smalley, R. E. Nature 318, 162–163 (1985).
2. Zhang, Q. L. et al. J. phys. Chem. 90, 525–528 (1986).
3. Liu Y. et al. Chem. Phys. Lett. 126, 215–217 (1986).
4. Bochavar, D. A. & Gal'pern, E. G. Dokl. Acad. Nauk SSSR, Chem., Engl. 209, 239–241 (1972).
5. Davidson, R. A. Theor. chim. Acta 58, 193–231 (1981).
6. Haymet, A. D. J. Chem. Phys. Lett. 122, 421–424 (1985); J. Am. chem. Soc. 108, 319–321 (1986).
7. Klein, D. J., Schmalz, T. G., Hite, G. E. & Seitz, W. A. J. Am. chem. Soc. 108, 1301–1302 (1986).
8. Newton, M. D. & Stanton, R. E. J. Am. chem. Soc. 108, 2469–2470 (1986).
9. Disch, R. L. & Schulman, J. M. Chem. Phys. Lett. 125, 465–466 (1986).
10. Haddon, R. C., Brus, L. E. & Raghavachari, K. Chem. Phys. Lett. 125, 459–464 (1986).
11. Haddon, R. C. Aust. J. Chem. 30, 1–22 (1977).
12. Haddon, R. C. J. Am. chem. Soc. 101, 1722–1728 (1979).
13. London, F. J. Phys. Rad. 8, 397–409 (1937).
14. Haddon, R. C. J. Am. chem. Soc. (submitted).
15. Haddon, R. C. Tetrahedron 28, 3613–3634, 3635–3655 (1972).
16. Kuwajima, S. & Soos, Z. G. J. Am. chem. Soc. 108, 1707–1708 (1986).
17. DiSalvo, F. J., Safran, S. A., Haddon, R. C., Waszczak, J. V., Fischer, J. E. Phys. Rev. B 20, 4883–4888 (1979).
18. Haigh, C. W. & Mallion, R. B. in Progress in NMR Spectroscopy (eds Emsley, J. W., Feeney, J. & Sutcliffe, L. H.) Vol. 13, 303–344 (Pergamon, Oxford, 1979).
19. Garratt, P. J. Aromaticity (Wiley, New York, 1986).
20. Salem, L. Molecular Orbital Theory of Conjugated Systems, Ch. 3 (Benjamin, New York, 1966).
21. Aihara, J.-I. Bull. chem. Soc. Japan 53, 1751–1752 (1980).
22. McWeeny, R. Molec. Phys. 1, 311–321 (1958).
23. Elser, V. & Haddon, R. C. Phys. Rev. A (submitted).
24. Pauling, L. J. chem. Phys. 4, 673–677 (1936).

A new method for measuring the surface energy of solids

K. Kendall, N. McN. Alford & J. D. Birchall

ICI New Science Group, PO Box 11, The Heath, Runcorn, Cheshire WA7 4QE, UK

Although the surface tension of liquids has been understood and measured since the time of Young[1] and Laplace[2], the surface energy of solids has eluded understanding and evaded measurement, despite its postulated importance to catalysis, crystal growth, colloidal behaviour, sintering and fracture. It is salutary to reflect that solid surface energies are even now more readily determined by theoretical argument than by experiment. Here we show that solid surface energies can be evaluated experimentally by measuring the elastic modulus of submicrometre powder assemblies, knowing the particle diameter, elastic modulus and volume fraction.

The problem is that solids should display higher surface energies than liquids, but their atoms are relatively immobile, so that stresses in the surface may exist in addition to the surface tension of the solid. Attempts to distinguish the genuine solid surface tension from such spurious stresses have not been satisfactory[3,4]. For the same reason experiments to find the surface energy of the solid by measuring the enhanced vapour pressure[5], increased solubility[6], enlarged heat of dissolution[7] or lowered melting point[8] of powders have had only limited success; other energy terms shroud the surface contribution to such an extent that the very existence of solid surface energy has been doubted[5].
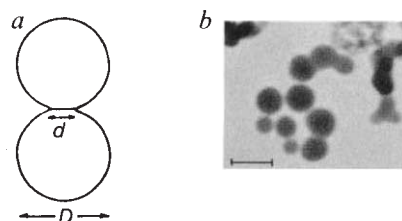

Fig. 1 a, Two elastic, smooth spheres in contact under zero external load form a contact spot of diameter d. b, Transmission electron micrograph of silica particles (OX50, Degussa). Scale bar, 0.1 μm.

Similar obstacles have dogged the cleavage method, the most popular way of estimating solid surface energies since Griffith[9] proposed his criterion of brittle fracture and Obreimoff[10] showed the importance of gaseous contamination. Although cleavage experiments have given results close to the theoretically expected values[11], it is more usual to obtain inordinately high figures because plastic flow occurs under the high stresses near the crack tip, even for brittle materials, causing a large and indeterminate energy demand[12].

Our new method avoids this difficulty because it is an equilibrium measurement which does not involve cleavage. Instead it is a development of the method devised for rubber, measuring the equilibrium diameter of the contact between two solid bodies held together by surface forces[13]. The interfacial energy between two plane surfaces of unit area was defined as Γ, the energy released on bringing the surfaces from infinity into contact. For identical solids, Γ was twice the surface energy of each piece, $\Gamma = 2\gamma$.

Experimentally, it proved better to use spheres rather than plane surfaces and to measure the enlargement of the Hertz[14] elastic contact circle by the attractive surface forces[15–19]. The interface energy Γ was then calculated from the equation

$$d^3 = 3(1-\nu^2)\frac{D}{E}\left[W + \frac{3}{4}\pi D\Gamma + \sqrt{\frac{3}{2}\pi DW\Gamma + \left(\frac{3}{4}\pi D\Gamma\right)^2}\right] \quad (1)$$

where d was the contact spot diameter, W the external load on the spheres, D the sphere diameter, E its Young's modulus and ν its Poisson's ratio. It was demonstrated that this method gave a better approach to equilibrium than a fracture test on the same geometry[13]. For 44 mm diameter rubber spheres the interfacial energy was measured to be $\Gamma = 71$ mJm^{-2} falling to 6.8 in water and to less than 1 mJm^{-2} in a 0.01 molar solution of sodium dodecyl sulphate. These values, inserted in Young's equation, were consistent with contact angle determinations. The main problem was surface roughness, inhibiting molecular contact and restricting the method to 'smooth' solids such as rubber or mica[20] which satisfied a smoothness criterion[21] depending largely on the centre line average roughness and the elastic modulus of the sample. Large spheres of ceramics would require almost atomically smooth surfaces to produce an adhesive contact.

In this report we recognize that this restriction of solid smoothness applies only to large bodies. It has previously not been observed that equation (1) should apply to all solids if the sphere size is made sufficiently small. In the limit, a single atom cannot be rough. Similarly, a 10 nm diameter particle should appear smooth as far as adhesion is concerned. Although the upper bound to this argument has not been defined (because Fuller and Tabor[21] only addressed the contact of plane surfaces, following Johnson[22]) it is reasonable to suppose that equation (1) should hold for ceramic grains less than 1 μm in size. Particles of this kind are found to adhere to a considerable degree[23]. The snag in using such particles to measure surface energy is that the contact spot is only tens of nm in diameter. Electron microscopy proved useful in defining the contact for metal and polymer latex spheres[24,25]. Here it is shown that the contact spot
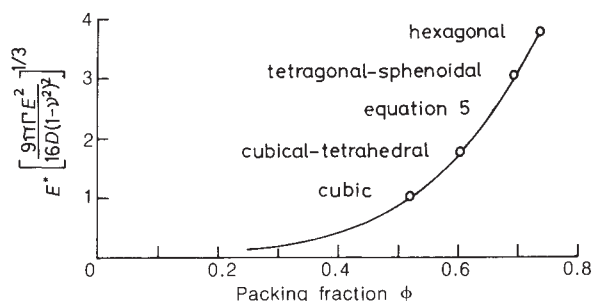
Fig. 2 Calculated elastic modulus for four regular sphere packings for comparison with equation (5).

Fig. 3 *a*, Elastic modulus results for particle assemblies compared with equation (5). ○, Titania powder, mixed in polymer solution. □, Titania powder, die pressed, $\Gamma = 0.6$ Jm^{-2}. +, Silica powder, $\Gamma = 0.05$ Jm^{-2}. *b*, Results for silica powders of different particle diameter compared to equation (5). The broken line shows equation (5) plotted for $\Gamma = 1.16$ Jm^{-2}, a theoretical estimate for pure silica[25]. The other line shows equation (5) plotted for $\Gamma = 0.05$ Jm^{-2}.

size may be determined from the elastic modulus of a powder assembly[26] allowing the interfacial energy Γ to be calculated.

Consider two equal spheres in contact under zero external load (Fig. 1*a*). The diameter of the contact spot from equation (1) is

$$d = \left[\frac{9\pi}{2E} \Gamma D^2 (1 - \nu^2) \right]^{1/3} \quad (2)$$

This can be measured by applying a small test load P and following the elastic deformation δ of the spheres since[13]

$$P/\delta = Ed/2(1 - \nu^2) = \left[\frac{9\pi \Gamma E^2 D^2}{16(1 - \nu^2)^2} \right]^{1/3} \quad (3)$$

Although the deformation at a single contact is minute, it can be magnified by stacking the spheres end to end in a regular cubic packing, whose elastic modulus E^* from equation (3) is

$$E^* = P/d\delta = \left[\frac{9\pi \Gamma E^2}{16 D(1 - \nu^2)^2} \right]^{1/3} \quad (4)$$

To judge the effect of changing the packing from simple cubic, the elastic modulus was also calculated for hexagonal close packing and for two other regular packings of uniform spheres. It was found that the elastic modulus increased with packing fraction ϕ (volume of spheres/volume of assembly) along a single curve (Fig. 2) described by

$$E^* = 17.1 \, \phi^4 \left[\frac{\Gamma E^2}{D} \right]^{1/3} \quad (5)$$

Qualitatively, this ϕ^4 dependence of E may be understood in terms of two effects; first the ϕ^2 dependence of modulus on the density of particle packing[27]; second, a further ϕ^2 dependence of modulus on the coordination number of each sphere[28]. Based on this simple reasoning, it was proposed that irregular sphere packings should also fall on this same curve.

The following experiments were designed to test this hypothesis and then to use equation (5) to measure the interface energy Γ of ceramic particles. Silica (OX50, Degussa, $D = 0.05 \, \mu$m, $E = 70$ GPa) (Fig. 1*b*) and titania (RCR2, Tioxide, $D = 0.23 \, \mu$m, $E = 280$ GPa) were used to make the particle assemblies because they were nearly spherical and of relatively narrow size distribution. The particles were mixed in a polymer solution (30% polyvinyl alcohol (KH 17 s, Nippon Gohsei) in water) pressed to a sheet, dried, cut into strips, then heated to 500 °C to remove the polymer. The resulting particle assemblies were bend tested to determine Young's modulus E^* which was plotted against packing fraction ϕ derived from the weight and volume of the strip.

The measurements for titania (Fig. 3*a*) gave a good fit to the ϕ^4 relation of equation (5) and correspond to a value of $\Gamma = 0.6$ Jm^{-2} reasonably close to the theoretical estimate of $\Gamma = 0.8$ Jm^{-2} for the 110 plane of rutile at 20 °C[29]. A powder compact made by pressing in a steel die gave a result near the curve, indicating that the modulus was not strongly affected by the preparation method. Possible errors in the experimental results
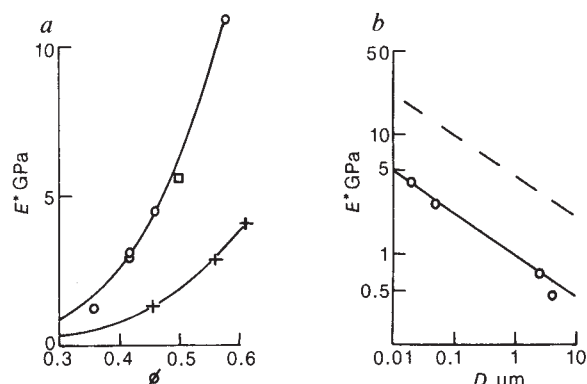
stem from inaccuracy of particle diameter determination, the spread of particle sizes in the powder and anisotropy of particle shape and elasticity.

Results for silica also fitted equation (5) but corresponded to $\Gamma = 0.05$ Jm^{-2}, much lower than the theoretical 1.16 Jm^{-2} for the 110 plane of β cristobalite[29]. This low value was confirmed by additional measurements on a series of pure silica powders of different diameter, results which supported the $D^{-1/3}$ dependence of modulus (Fig. 3*b*). The low result for Γ was unchanged when the silica assembly was immersed in water, suggesting that the silica surface was already saturated by atmospheric contamination. Heating the silica to 700 °C gave a weight loss of almost 1% and increased the modulus by a factor of nearly 2, indicating that water was being driven off to increase the surface energy of the silica. On cooling and rewetting, the modulus fell back again. This observation is important to ceramics, which require low surface energy to ease powder compaction[30] but a high surface energy to drive sintering at elevated temperatures.

In conclusion, the surface energy of solids may be measured by determining the elastic modulus of fine powder assemblies, knowing the packing fraction, the diameter and the elastic properties of the grains. Although there are difficulties because many powders are not spherical, uniform or isotropic, it is believed that this new method may make the surface energy of solids as experimentally accessible as that of liquids, adding to our knowledge and application of surface phenomena.

1. Young, T. *Phil. Trans R. Soc.* **95**, 65–87 (1805).
2. Laplace, P. S. *Mecanique Celeste* Suppl Book 10 (translated by Bowditch, N.) 685–1018 (Chelsea Publishing, New York, 1966).
3. Chapman, J. C. & Porter, H. L. *Proc. R. Soc.* A83, 65–68 (1910).
4. Berggren, B. *Ann. Phys.* **44**, 61–80 (1914).
5. Bikerman, J. J. *Phys. Status Solidi* **10**, 3–25 (1965).
6. Alexander, G. B. *J. phys. Chem.* A171, 1563–1564 (1957).
7. Benson, G. C., Schreiber, H. P. & van Zeggeren, F. *Can. J. Chem.* **34**, 1553–1556 (1956).
8. Sill, R. C. & Skapski, A. S. *J. chem. Phys.* **24**, 644–651 (1956).
9. Griffith, A. A. *Phil. Trans. R. Soc.* A221, 163–198 (1920).
10. Obreimoff, J. W. *Proc. R. Soc.* A127, 290–297 (1930).
11. Gilman, J. J. *J. appl. Phys.* **31**, 2208–2218 (1960).
12. Lawn, B. R. & Wilshaw, T. R. *Fracture of Brittle Solids*, Ch. 6 (Cambridge University Press, Cambridge, 1975).
13. Johnson, K. L., Kendall, K. & Roberts, A. D. *Proc. R. Soc.* A324, 301–313 (1971).
14. Hertz, H. J. *Reine angew. Math.* **92**, 156–171 (1882).
15. Tabor, D. *J. Colloid. Interface Sci.* **58**, 2–13 (1977); **67**, 380 (1978); **73**, 294 (1980).
16. Derjaguin, B. V., Muller, V. M. & Toporov, Y. P. *J. colloid Interface Sci.* **53**, 314–326 (1975); **67**, 378–379 (1978); **73**, 293 (1980).
17. Muller, V. M., Derjaguin, B. V. & Toporov, Y. P. *Colloids Surfaces* **7**, 251–259 (1983).
18. Pashley, M. D. *Colloids Surfaces* **12**, 69–77 (1984).
19. Horn, R. G., Israelachvili, J. N. & Pribac, F. *J. colloid Interface Sci.* (in the press).
20. Maugis, D. & Barquins, M. in *Adhesion and Adsorption of Polymers* (ed. Lee, L.) 203–277 (Plenum, New York, 1980).
21. Fuller, K. N. G. & Tabor, D. *Proc. R. Soc.* A345, 327–342 (1975).

22. Johnson, K. L. *Proc. IUTAM Symp. on The Mechanics of Contact between Deformable Bodies* (eds de Pater & Kalker) 26–40 (Delft University Press, 1975).
23. Kendall, K., Alford, N. McN. & Birchall, J. D. *Spec. Ceram.* **8**, 255–265 (Institute of Ceramics, Stoke-on-Trent, 1986).
24. Easterling, K. E. & Thölen, A. R. *Acta met.* **20**, 1001–1008 (1972).
25. Kendall, K. & Padget, J. C. *Int. J. Adhesion Adhesives* July, 149–154 (1982).
26. Kendall, K., Alford, N. McN. & Birchall, J. D. *Proc. R. Soc.* (submitted).
27. Holliday, L. *Composite Materials* Ch. 2 (Elsevier, London, 1966).
28. Norman, L. D. & Maust, R. *Bull. U.S. Bur. Mines* **58**, 35–48 (1971).
29. Bruce, R. H. *Sci. Ceram.* **2**, 359–367 (1966).
30. Kendall, K. *Nature* **319**, 203–205 (1986).

Mechanical instability of gels at the phase transition

Toyoichi Tanaka, Shao-Tang Sun, Yoshitsugu Hirokawa, Seiji Katayama, John Kucera, Yoshiharu Hirose & Takayuki Amiya

Department of Physics and Center for Materials Science and Engineering, Massachusetts Institute of Technology, Cambridge, Massachusetts 02139, USA

Polymer gels, consisting of a cross-linked polymer network immersed in liquid, undergo a volume phase transition: when external conditions such as temperature or solvent composition change, a gel reversibly swells or shrinks, but does so discontinuously[1–5]. The volume change at the transition can be as large as a factor of one thousand[2], and the phenomenon occurs in all gels[6,7]. The equilibrium aspects of the phase transition have been extensively studied, but its kinetics have not yet been fully explored. In particular, the appearance of patterns on the originally smooth surface of a gel during the transition makes the kinetic process difficult to understand. Here we elucidate the physical basis underlying the formation and evolution of the pattern.

When a polymer gel undergoes an extensive swelling, a beautiful, regular pattern appears on the surface of the gel (as shown on this week's cover). At the beginning, the pattern is extremely fine, having a texture similar to that of a frosted glass. As time goes on, the units of pattern coalesce, doubling their characteristic size. When the unit size becomes comparable to the size of the gel, the pattern gradually disappears. As the gel approaches equilibrium, it regains the shape identical to the original one. Finally the gel becomes totally homogeneous, and the process comes to an end.

The pattern is formed in all the gels we have studied, that is, some polyvinyl gels and gels made of natural polymers. We chose ionized acrylamide gels because of their relative ease of handling. Copolymeric gels of acrylamide (700 mM) and sodium acrylate (0–32 mM) are prepared by a standard method using free radical polymerization initiated by ammonium persulphate and catalysed by tetramethylethylenediamine[1]. The osmotic pressure of counterions from sodium acrylate exerts an internal osmotic pressure and causes the gel to expand when placed in water. The volume expansion increases with the amount of sodium acrylate. The gel has a radius ~2 cm before swelling and 8 cm after complete swelling. The gel has a perfectly smooth surface before swelling, and as the gel is placed in water an extremely fine pattern appears on the surface[8]. As time goes on, the unit size of the pattern becomes larger by coalescence of units into a larger unit, which is accomplished by conversion of side lines into thorns followed by the disappearance of thorns. Eventually the size of the unit becomes comparable to that of the gel radius, when the pattern disappears completely. It continues to swell to the final volume until it regains the spherical shape and totally homogeneous density.

Careful observation shows that the pattern consists of numerous line segments of cusps into the gel. These cusps are not due to breaking of the gel, nor are the representative of a shrunken portion of the gel. The line is a result of shear bending of a homogeneously swollen gel surface. Indeed, when the surface is sliced off in a thin layer, the pattern disappears instantly, and the slice becomes homogeneous. If the cusps were due to local shrinking of the gel, they would take a long time to disappear through the collective diffusion process. At each swelling stage, the pattern appears to be a hexagonal lattice, but it is quite irregular. A similar pattern is observed on the surface of the acrylamide gel formed in a Petri dish and swollen in water (Fig. 1). The patterns are formed only when swelling is extensive: if the swelling is small, the surface of the gel remains smooth throughout the entire process.

The pattern formation may be qualitatively explained in the following way. The kinetic process of the swelling of a gel is governed by the collective diffusion of the polymer network into a solvent[9]. At first, a very thin surface layer is swollen. This layer is under a mechanical constraint, namely, the outer surface of the layer is free to expand, whereas the inner surface is fixed to the core of the gel. Thus, the layer is under opposing demands on the upper and lower surfaces, one to expand and the other to remain unswollen. When the osmotic pressure is small, these opposing forces are resolved by stretching the gel unidirectionally perpendicular to the surface. When the osmotic pressure is large the outer surface is forced to buckle. The characteristic wavelength of the pattern must be proportional to the thickness
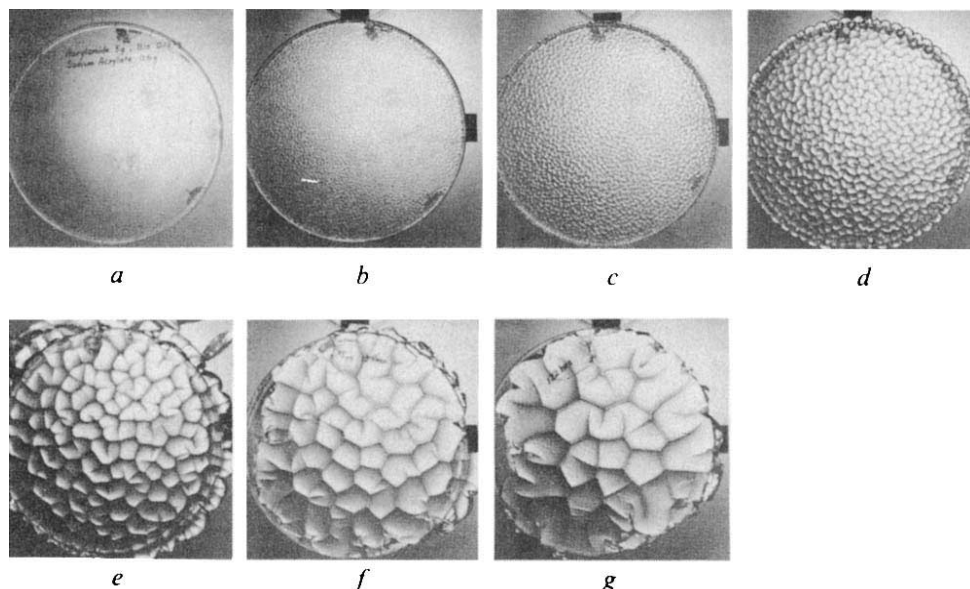

Fig. 1 An ionized acrylamide gel formed in a Petri-dish is allowed to swell in water. An extremely fine pattern appears on the free surface of the disk gel, and evolves with time (a → g).